Experimental And Modeling Analysis Of Internal Luminescence In III-V Solar Cells

Myles A. Steiner, John F. Geisz, Iván García, Daniel J. Friedman, Sarah R. Kurtz

Abstract: In high quality solar cells, the internal luminescence can be harnessed to enhance the overall performance. Internal confinement of the photons can lead to an increased open-circuit voltage and short-circuit current. Alternatively, in multijunction solar cells the photons can be coupled from a higher bandgap junction to a lower bandgap junction for enhanced performance. We model the solar cell as an optical cavity and compare calculated performance characteristics with measurements. We also describe how very high luminescent coupling alleviates the need for top-cell thinning to achieve current-matching.

Keywords: III-V solar cell, luminescence, radiative coupling, top-cell thinning

The electrical properties of a solar cell are paramount in determining the conversion efficiency, but in direct bandgap cells with very good material quality so are the internal optics. Radiative recombination of electron-hole pairs leads to the emission of photons which, if confined by good reflectors at the front and back of the cell, can be reabsorbed and re-emitted, ultimately increasing the equilibrium minority carrier lifetime and the open-circuit voltage, V_{oc}.[1, 2] If those spontaneously emitted photons are not confined but rather are absorbed by a lower bandgap junction in a multijunction cell, the resulting luminescent coupling will increase the photocurrent of the lower bandgap junction.[3, 4] In both cases the overall conversion efficiency will increase, relative to the case where the photons are lost. Optical effects can therefore have important consequences for the design and measurement of multijunction solar cells. Here, we present a combined experimental and modeling analysis of the consequences of these effects in actual solar cells, and we demonstrate that the impact on cell design and performance can be significant.

To understand the influence of the optics, it is useful to think of the solar cell as an optical cavity where photons can reflect multiple times off the various interfaces and possibly interfere with each other. For thick solar cells it is generally sufficient to treat the cavity with ray optics in which only the intensity of the light varies with location. The optical cavity must have a high absorbance so that most of the incoming light is converted into electron-hole pairs. But the optical cavity must also manage the internal luminescence: while some of the internally emitted photons will escape out the front of the cell or be re-absorbed parasitically in the various cladding layers or in the substrate, a significant fraction of the photons will be reabsorbed in the active layer and reincarnated as new electron-hole pairs. This so-called "photon recycling" increases the effective minority carrier lifetime, which in a solar cell leads to an increase in the quasi-Fermi level separation and therefore the V_{oc}.

The cavity nature of the cell can be clearly observed in the external quantum efficiency (EQE) of thin, high quality GaAs cells, as shown in Fig. 1. Both cells shown are 1 μm thick and were intentionally not covered with an anti-reflection coating.

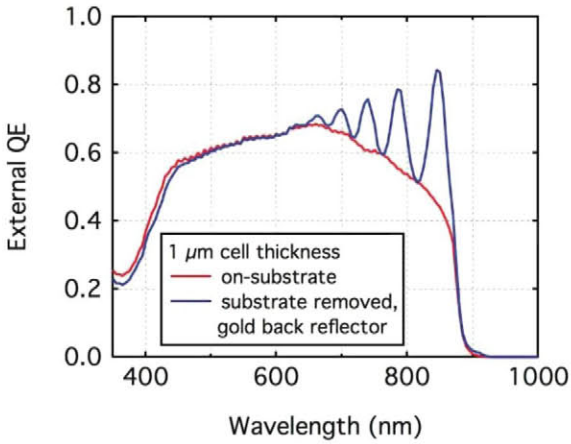

FIGURE 1. Measured EQE for two 1-μm GaAs solar cells without anti-reflection coatings. The blue curve is for a cell where the substrate was removed after growth and replaced with a highly reflective gold back contact.

The red curve is for a standard cell on the substrate and shows incomplete photon absorption because the cell is substantially thinner than the ~3.5-μm optical thickness for GaAs. The blue curve is for a cell where

the substrate was removed and replaced with a highly reflective gold mirror. Normally incident light reflects off the back and passes through the cell a second time, and because the front surface is not AR-coated, ~35% of that light also reflects internally off the front interface and passes through the cell again. The cell is therefore a Fabry-Perot optical cavity, exhibiting strong interference fringes between forward- and backward-traveling light waves.

A description of the internally emitted light is complicated by the isotropic nature of the emission, and care must be taken to account for the different pathlengths through the absorber at each angle of emission. Our full model is described in detail in Ref. 1; here we summarize the derivation and conclusions.

On thermodynamic grounds, the V_{oc} can be described as[5]

$$V_{oc} = V_{db} + \frac{kT}{q}\ln(\eta_{ext}) \qquad (1)$$

where V_{db} is the ideal open-circuit voltage calculated in the detailed balance limit where there are no non-thermodynamic losses, and η_{ext} is the external luminescent efficiency that quantifies the fraction of electron-hole pairs that lead to internally emitted photons that are ultimately able to escape through the front surface. In essence, all of the electrical and optical losses in the cell are aggregated into η_{ext}, which then represents the total loss in voltage. V_{db} can be calculated directly from the EQE.[6] η_{ext} can be calculated by observing that an internally emitted photon can escape the cell directly, or it can be reabsorbed and re-emitted and then escape, or reabsorbed again etc. These possibilities are sketched in Fig. 2.

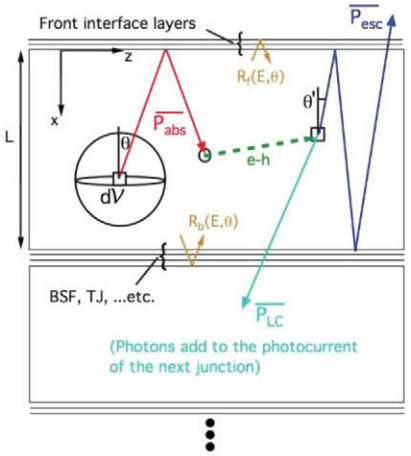

FIGURE 2. Geometry of the optical cavity model. Photons are emitted from the differential volume $d\mathcal{V}$, and can be re-absorbed (red), emitted out the front (dark blue), coupled to a lower bandgap junction (light blue), or absorbed parastically during a reflection (yellow). The dashed green line indicates diffusion of an electron-hole pair.

Summing over all of the possibilities, and accounting for the different optical pathlengths at each emission angle, we find

$$\eta_{ext} = \frac{\eta_{int}\overline{P_{esc}}}{1 - \eta_{int}\overline{P_{abs}}}, \qquad (2)$$

where $\overline{P_{esc}}$ represents the average probability that a photon escapes before being reabsorbed (blue pathway), $\overline{P_{abs}}$ represents the average probability that a photon is reabsorbed (red pathway), and η_{int} is the internal luminescent efficiency, or the probability that an electron-hole pair recombines radiatively, which is a useful metric for the overall material quality. We assume here that η_{int} is uniform throughout the cell volume, which is reasonable for modern, high quality cells. $\overline{P_{esc}}$ and $\overline{P_{abs}}$ are complicated functions of the geometry and the angle- and wavelength-dependent Fresnel coefficients at the front and back, and expressions are given in Ref. 1.

The optical cavity is designed to maximize η_{ext}, which for real cells can be achieved by increasing any of the three quantities in Eq. (2). From the perspective of the cell design, the optical design is most sensitive to the reflectances at the front and back of the cell and to the cell thickness. The angle-averaged front reflectance is high because of total internal reflectance, though an anti-reflection coating will reduce the near-normal reflectance. A high back reflectance can be achieved by removing the substrate and depositing a reflective metal such as gold or silver, or a dielectric/metal bilayer. Figure 3 shows the measured V_{oc} for a 2-μm thick GaAs cell, with and without an anti-reflection coating, as a function of the thickness of an absorbing GaAs back contact layer: the primary function of the contact layer is to enable Ohmic contact between the electroplated gold and the semiconductor, but the layer can also serve a secondary purpose of lowering the overall reflectance by absorbing some of the luminescence, to allow a systematic exploration of the optical effects.

The measurements show that V_{oc} increases by ~5 mV after application of the ARC, as predicted, but in both cases decreases by ~20 mV when the GaAs contact layer thickness increases from 10 nm to 3000 nm. The solid lines show modeling of V_{oc} following Eqs. (1) and (2), for three different values of η_{int}. The data are reasonably modeled by $\eta_{int} = 0.965$ with and without the ARC—it is expected that the internal luminescent efficiency should be unchanged by the ARC.

Several important conclusions can be drawn from Fig. 3. V_{oc} is clearly more sensitive to the back reflectance in cells of high material quality, as can be seen from the different slopes of the lines with $\eta_{int} = 1$ and 0.7. Conversely, improved material

quality has a more pronounced effect on the performance in cells with good optical properties than with poor optical properties. Finally, in this model of a solar cell where the internal luminescent efficiency is uniform, the optical and non-radiative recombination losses are separable, as indicated by the vertical arrows. Even for a cell with perfect material quality, $V_{oc} < V_{db}$ because of the parasitic optical losses at each reflection.

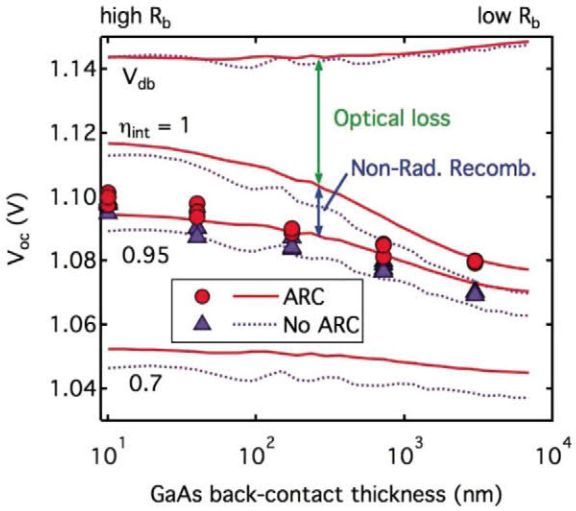

FIGURE 3. Modeled (lines) and measured (points) V_{oc} for a 2-μm GaAs cell. The rear contact consists of a layer of GaAs of variable thickness, followed by an electroplated gold mirror. The purple and red lines/points correspond to uncoated and coated cells, respectively. The lines at the top show V_{db} as calculated from the EQE. η_{int} is indicated.

The model described above can be applied to each junction in a multijunction solar cell, with the various other layers in the structure all contributing to the calculation of the Fresnel coefficients for a particular junction. Thus, for example, the calculated value of η_{ext} for our best 2-μm GaAs cell is 17.6%, and if that cell were covered with a 1-μm GaInP top junction, η_{ext} would drop slightly to 16.4%, corresponding to a drop in V_{oc} of only ~2 mV.

The same model can also be used to calculate the external luminescent efficiency out the back of an upper junction by interchanging $R_b \leftrightarrow R_f$ and $T_b \leftrightarrow T_f$ in the expression for $\overline{P_{esc}}$, and thereby calculating the luminescent coupling efficiency between two junctions. Replacing $\overline{P_{esc}}$ with the analagous $\overline{P_{LC}}$ (light blue pathway in Fig. 2) the coupling efficiency is then given by

$$\eta_{12} = \frac{\eta_{int}\overline{P_{LC}}}{1 - \eta_{int}\overline{P_{abs}}} \qquad (3)$$

and can be compared directly to measurements.

As shown in Ref. 3, the actual coupling constant can be measured on an adjustable solar simulator by using the variable illumination to force the cell into different current-limiting configurations. The relative intensity on each junction and the short-circuit current through the tandem are measured at each illumination condition. The coupling parameters and externally induced one-sun photocurrents are then deduced by fitting all of the data to an analytical model. We used a class A solar simulator with light from a xenon lamp and LEDs with wavelengths 470, 850 and 940 nm. Matched and calibrated reference cells were used to determine the relative intensity on each junction, and the total spectrum at each illumination condition was measured by a Spectral Evolution photoradiometer, in order to correct for spectral mismatch.

Figure 4 shows the effects of luminescent coupling on a series of two-junction GaInP/GaAs tandem cells in which we artificially lowered the coupling by thickening an absorbing $Al_{0.2}Ga_{0.8}As$ layer grown between the two junctions. The EQE in Fig. 4a shows that the top junctions are unaffected by the change but the bottom junctions show a decreasing absorption near 700-750 nm. The EQEs of the bottom junction have been corrected for luminescent coupling following the method in Ref. 4.

In Fig. 4b, the modeled coupling constant is shown for four different values of the internal luminescent efficiency of the top junction. The measured data, shown in red, are all consistent with $\eta_{int} \sim 80 - 85\%$ even as the magnitude of the coupling drops by a factor of two, from 0.52 for the 50 nm barrier to 0.27 for the 300 nm barrier. Separate measurements (not shown) of single junction GaInP cells with the same layer structure are also consistent with $\eta_{int} \sim 80\%$. Thus the coupling between junctions can be reasonably well modeled.

Luminescent coupling in a multijunction solar cell can be beneficial to the overall performance, and indeed must be considered when designing the structure. In a bottom-limited tandem (for two junctions) the coupling raises the photocurrent of the bottom junction and represents a recovery of photocurrent that would otherwise be lost if those photons were simply absorbed parasitically. This affects the top-cell thinning design rule.[7]

The top junction is often thinned so that some of the photons that should be absorbed there are instead absorbed in a lower junction, because tandems generally operate most efficiently when the equilibrium photocurrents of each junction are matched. In a bottom-limited tandem, some of those photons can be transferred through luminescent coupling, alleviating to some extent the need to thin the top cell.

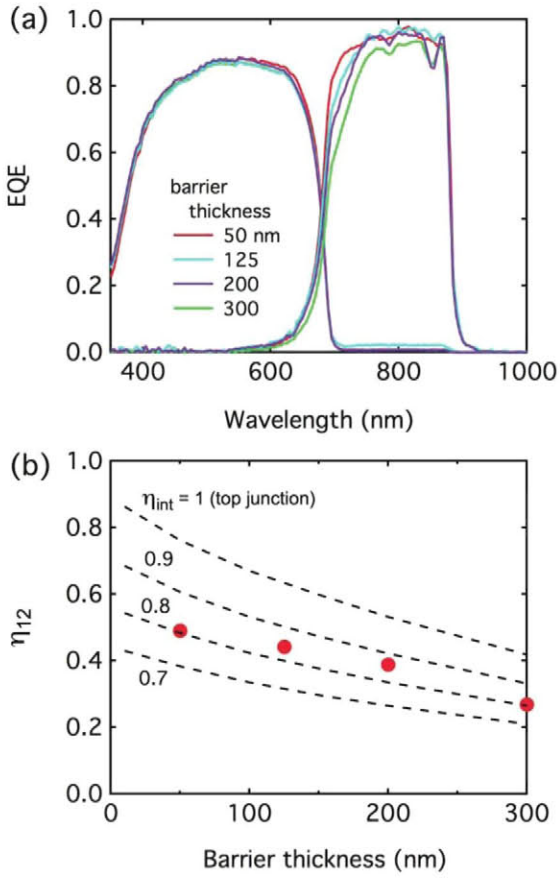

FIGURE 4. Luminescent coupling in a GaInP/GaAs tandem cell. The coupling was tuned by changing the thickness of an absorbing $Al_{0.2}Ga_{0.8}As$ diffusion barrier layer grown between the two junctions. (a) EQE corrected for luminescent coupling. (b) Measured values of the coupling constant η_{12} as defined in Refs. 3 and 4, and calculated values using four choices of the top junction internal luminescent efficiency, η_{int}.

Figure 5 shows the calculated conversion efficiency for a two-junction tandem cell as function of the top junction thickness. The cell was similar to the structure studied in Fig. 4 but with a higher bandgap $Al_{0.3}Ga_{0.7}As$ barrier layer instead of $Al_{0.2}Ga_{0.8}As$. For each value of the top junction thickness, the optical cavity model was used to calculate $\overline{P_{esc}}$, $\overline{P_{abs}}$ and V_{db} for both junctions, as well as $\overline{P_{LC}}$ for photons escaping out the back of the top junction, and the externally induced J_{sc}s for each junction. We used $\eta_{int} = 0.965$ for the internal luminescent efficiency of the bottom junction, and the four values shown in the figure for the top junction. Eq. (2) was used to calculate the external luminescent efficiency for each junction, and the dark saturation currents were then calculated as

$$J_0 = \frac{J_{sc}}{\eta_{ext}} e^{-qV_{db}/kT}. \qquad (4)$$

If appropriate, the bottom junction photocurrent was modified to include a luminescent coupling current using Eq. (3) to calculate η_{12}. The JV curves were then added together and the total efficiency determined.

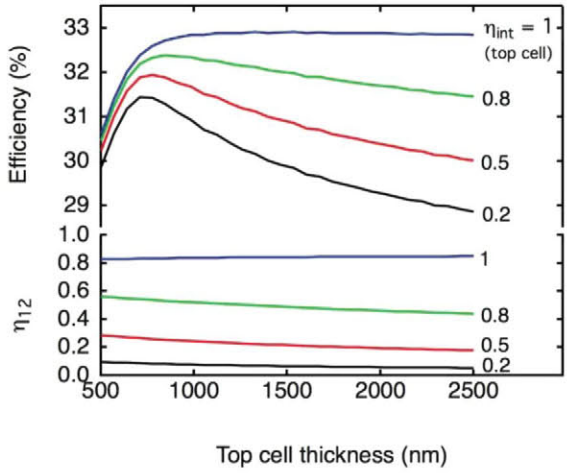

FIGURE 5. Effects of the top junction thickness on the conversion efficency of a GaInP/GaAs tandem, under the G173 direct solar spectrum at 1000 W/m^2. Calculations for four choices of the top junction η_{int} are shown; we assume $\eta_{int} = 0.965$ for the bottom junction. The bottom panel shows the calculated values of η_{12}.

The bottom panel of Fig. 5 shows the calculated values of η_{12}, where the coupling clearly increases as the top-junction η_{int} increases. The top panel shows that for low-to-moderate values of η_{12}, the efficiency is maximized at some optimum top-junction thickness. At $\eta_{12} \approx 0.8$, however, the efficiency saturates and *there is no longer any efficiency gain to be achieved by thinning*. In this particular cell, $\eta_{12} \approx 0.8$ is achieved with $\eta_{int} \approx 1$, but more transparent confinement, tunnel junction and diffusion barrier layers could enable the same coupling with imperfect material. Even at a material quality of $\eta_{int} = 0.8$ as was found for the cells in Fig. 4, the sensitivity to the top junction thickness is significantly less than for $\eta_{int} = 0.2$, which therefore increases the design flexibility.

Therefore, for the high quality multijunction cells that are currently being fabricated, the conventional top-junction thinning design rule may need to be relaxed in order to harness the power of the strong internal luminescence.

ACKNOWLEDGMENTS

The authors are grateful for conversations with E. Yablonovitch, C.-S. Ho, R. King, W. McMahon and R. France. Samples were prepared by W. Olavrria, M. Young and A. Duda. I. García holds a Fulbright postdoctoral scholarship funded by the Spanish Ministerio de Educación, by means of the Programa Nacional de Movilidad de Recursos Humanos del Plan Nacional de I-D+i 2008-2011. Research was supported by the U.S. Department of Energy under Contract No. DE-AC36-08GO28308 with the National Renewable Energy Laboratory and funded in part by the Foundational Program to Advance Cell Efficiency. This work is subject to government rights.

REFERENCES

1. M. A. Steiner, J. F. Geisz, I. García, D. J. Friedman, A. Duda and S. R. Kurtz, J. Appl. Phys. **113**, 123109 (2013).
2. O. D. Miller, E. Yablonovitch and S. R. Kurtz, J. Photovoltaics **2**, 303 (2012).
3. M. A. Steiner and J. F. Geisz, Appl. Phys. Lett. **100**, 251106 (2012).
4. M. A. Steiner, J. F. Geisz, T. E. Moriarty, R. M. France, W. E. McMahon, J. M. Olson, S. R. Kurtz and D. J. Friedman, J. Photovoltaics **3**, 879 (2012).
5. U. Rau, Physical Review B **76**, 085303 (2007).
6. E. S. Toberer, A. C. Tamboli, M. Steiner and S. Kurtz, in *38th IEEE Photovoltaic Specialists Conference* (IEEE, Austin, TX, 2012).
7. D. J. Friedman, J. F. Geisz and M. A. Steiner, submitted to J. Photovoltaics (2013).